Proceedings of the Forty first Turbomachinery Symposium
September 24-27, 2012, Houston, Texas

# Effectiveness of Windage Features on High Speed Couplings

**Steven Pennington**
Global Engineering Manager
John Crane Ltd
Manchester, UK

**Klaus-Dieter Meck**
Core Technology Manager
John Crane Ltd
Manchester, UK

*Steven Pennington is the Global Engineering Coupling Manager at John Crane, he manages a team of design engineers in Manchester controlling product standards and research and development. Products are verified using FEA and the technology lab containing static and dynamic test rigs able to recreate steady and cyclic conditions. Mr. Pennington has over 25 years of engineering experience in power transmission and rotating equipment. Mr. Pennington has a Mechanical Engineering degree from Manchester University, he is a Chartered Mechanical Engineer of the Institute of Mechanical Engineers*

*Klaus-Dieter Meck is the Core Technology Manager at John Crane R&D. Mr. Meck and his team support all product groups and develop enabling technologies for seals, power transmission couplings, engineered bearings and condition monitoring. Mr. Meck joined John Crane Ltd. in 1999 after previously working at Flexibox Ltd. During his 20 years in the industry he's been involved in product development and product application, supporting end users and OEM's. Mr. Meck is the author of several papers concerning sealing technology and rotating equipment. Mr. Meck received his Master Degree in* Mechanical Engineering from Stuttgart University, Germany.

## ABSTRACT

Following the changes to API 671, there is a requirement to reduce temperature around guarded coupling designs. Existing features used in high performance (HP) couplings involve various methods of shrouding and covering prominent rotating parts to ensure a smooth, rounded profile. The extent of the features are raised in line with increased peripheral speed. These key features are difficult and expensive to manufacture and can create high stress concentrations. This had lead to the investigation of the efficiency of the features. Traditional methods involve extensive test work, but due to the advances in computational fluid dynamics (CFD), the technology is now far more accessible to mainstream industry and can be used to analyze more complex coupling assemblies. This has allowed evaluation of windage features and their effect when rotated within a guard. Various geometric features have been analyzed using CFD and verified with test work, starting with a coupling equipped with all available windage features through to all of them removed. The initial results highlight that windage features fail to make a significant impact in reducing guard temperatures, hence further investigation has been planned.

## INTRODUCTION

Many industries invest significant time and effort reducing the temperatures within a guard assembly, especially at elevated temperatures and high peripheral speeds. API 671 fourth Edition, recommends the maximum guard temperature limit of 158°F (70°C), therefore the challenge is to reduce the several kilowatts of churning losses generated by a typical HP coupling.

Anti-windage features are an accepted and integrated part of the HP coupling design, but analysis has been limited to simple cylindrical models and testing. The flanges are difficult to manufacture and assembly is made harder by the flanges obscuring the tooling and fasteners. Designs incorporating many features increase the overall mass, especially when a shrouded design is used. Most of the manufactured features produced are long and slender and can create areas of high stress concentration which can be compounded by poor surface finish during machining. In some instances they have been known to be stimulated by adjacent components and introduced to resonance until eventual fatigue failure occurs.

The aim is to enable coupling geometry to reduce the effects of windage by outlining good and bad features and devise a numerical tool that can be used to optimize the guard and coupling geometry.

## SCOPE OF THE INVESTIGATION

The investigation presented is based around a typical high performance coupling, as shown in Figure 1. In order to access the efficiency of individual windage features, the guard diameter, distance between shaft ends and external environment conditions were fixed.

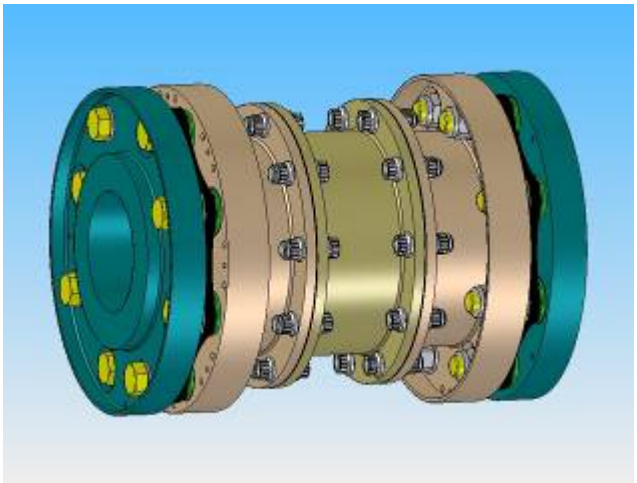

**Figure 1. CAD model of power transmission coupling.**

The investigation was conducted using CFD models of the coupling and its surroundings. In order to verify the accuracy of the CFD model, simulated performance data was correlated with test rig data presented in the empirical verification section.

With adaptive components, the typical environment of a high speed coupling was generated to simulate temperature and air flow conditions around the coupling and guard. The investigation was planned to study shaft speeds up to 10000rpm (equivalent to 200 m/s (660 fps)) at the coupling outer diameter.

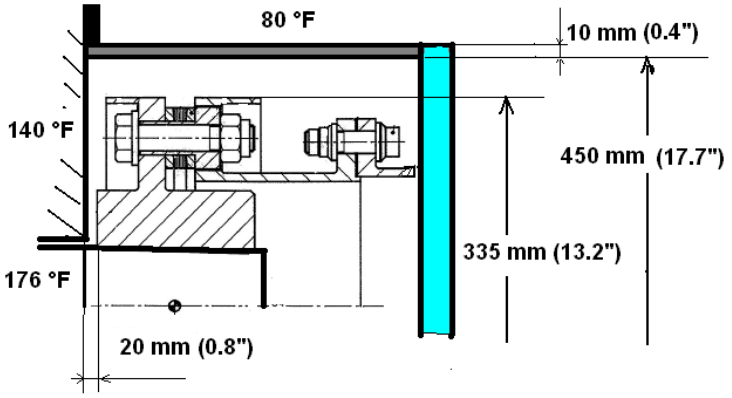


**Figure 2. Test setup-up and model boundary for CFD analysis.**

A matrix was developed that allowed the efficiency of the individual windage features to be analyzed with a minimum number of CFD runs, assuming that the affect of an individual feature regarding churning losses can be derived independently of other features, meaning that the individual windage features do not influence each other.

The total coupling configurations studied can be seen in Table 1, using conventional windage features, of which 3 configurations, numbers 2, 3 and 5, were tested.

**Table 1. Matrix for coupling windage feature investigation.**

| Config. | Clearance | No of Links | No Stripper Bolts | Drive Bolt Cover | Stripper Bolt Cover | Drive Bolt Cover Plate | Model |
|---|---|---|---|---|---|---|---|
| 1 | 3 | 8 | 16 | YES | YES | NO |  |
| 2 | 20 | 8 | 16 | YES | YES | NO | |
| 3 | 20 | 8 | 16 | YES | NO | NO |  |
| 4 | 20 | 8 | 16 | YES | YES | YES |  |
| 5 | 20 | 8 | 16 | NO | NO | NO |  |
| 6 | 20 | 8 | 8 | NO | NO | NO |  |
| 7 | 20 | 6 | 16 | NO | NO | NO |  |

The coupling configurations listed in the graphs are as follows:

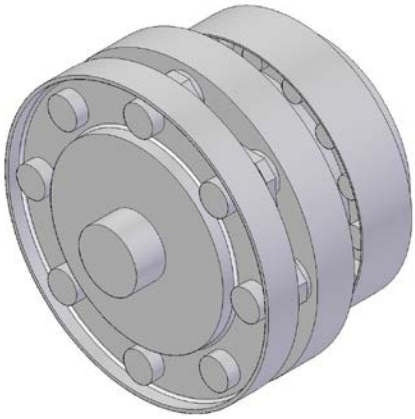

**Figure 3. Configuration 2.**

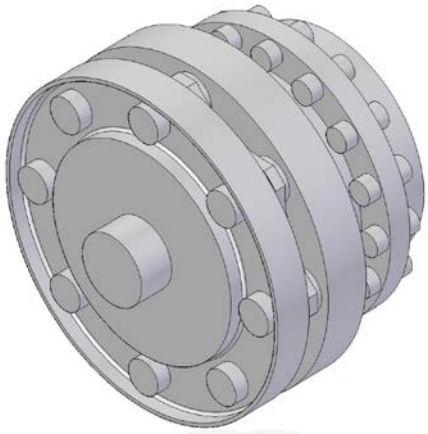

**Figure 4. Configuration 3.**

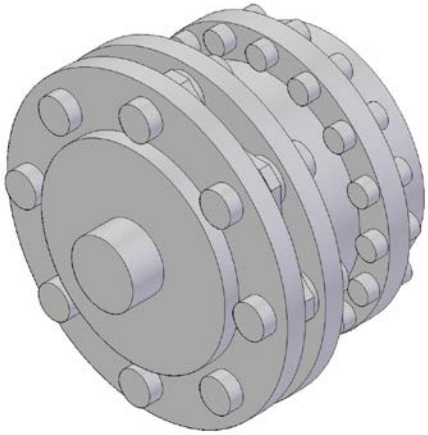

**Figure 5. Configuration 5.**

## CFD INVESTIGATION

*Analysis Model Setup*

The investigation was conducted using a commercially available CFD code by Ansys Inc. In order to manage the size of the CFD model, smaller design features such as bolts were simplified. Furthermore, geometrical symmetry was used to reduce the CFD model size and reduce the computational effort. In an independent CFD study it was established that geometrical symmetry can only be used up to a model size of a ¼ section of the coupling. For smaller sections the flow around the coupling is not symmetrical and therefore computed incorrectly, although geometrical symmetry exists. Figure 6 shows the CFD model and Figure 7 shows the correlation of the churning losses for 1/8 section, a 1/4 section and full section model.

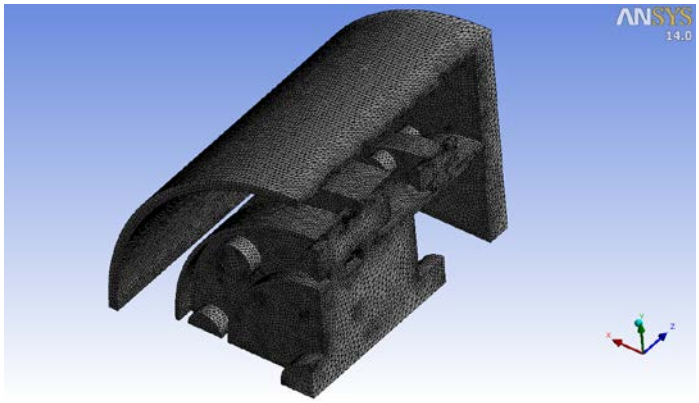


**Figure 6. CFD model using symmetry and model simplification.**

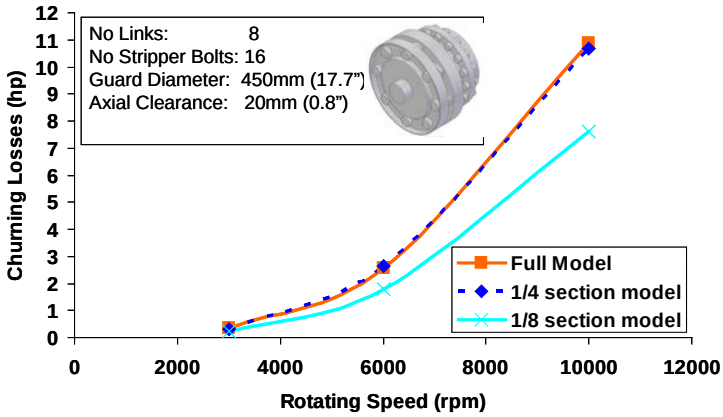


**Figure 7. Churning loss predictions and comparison between full and sectioned coupling CFD models, configuration 3.**

The presented CFD results were established by using a standard k-epsilon turbulence model. However, in order to verify the accuracy of the wall function of the k-epsilon turbulence model (which is fundamental to the accuracy of the churning loss prediction), simulations with a k-omega-SST turbulent model were conducted too. The churning loss prediction with both turbulence models agreed within an accuracy of more than 90%.

*Results*

By analyzing the flow around the coupling it was noted that losses are originated by either viscous drag at the coupling surfaces or flow separation around sharp object such as bolts or membranes. Conventional windage features as used with most HP membrane couplings are designed to cover areas of the coupling that have the potentially to cause flow separation. However, such features do in most cases increase the surface area of the coupling, thus, increasing losses associated to surface drag. Figure 8 shows the streamlines around the coupling with drive bolt covers and a coupling without any covers.

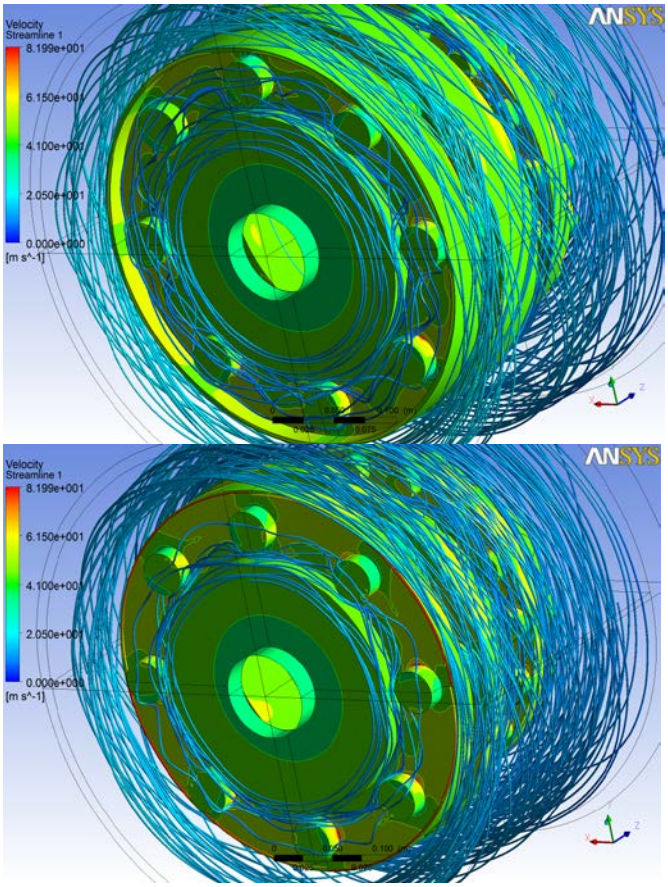


**Figure 8. Streamline for 4500 rpm around coupling configuration 3 (top) and configuration 5 (bottom).**

Figure 9 shows the effect of flow separation around the bolts manifesting itself in a compression zone at the leading part of the bolt (high pressure) and a wake region at the trailing end of the bolt (low pressure). Both pressure regions contribute to the losses associated with flow separation.

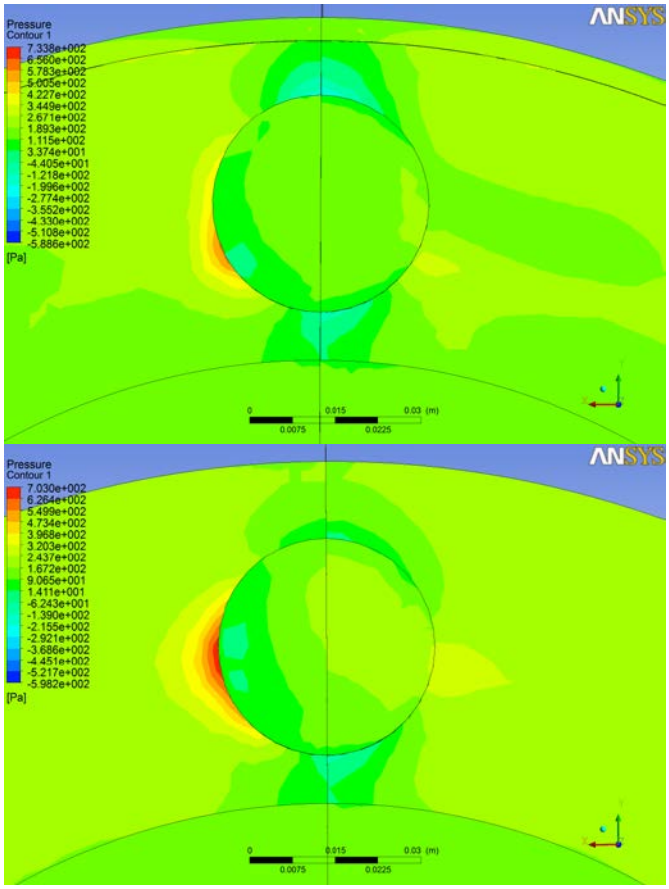


**Figure 9. Pressure distribution at the coupling drive bolts causing windage losses (4500 rpm, configuration 3 (top) and configuration 5 (bottom)).**

By analyzing the results in Figure 8 and 9, it can be observed that the flow streamlines and the losses at the drive bolts are similar in both cases. This suggests that the drive bolt cover windage feature is not efficient enough to eliminate the flow separation and therefore sufficiently reduce windage losses.

As all of the published results in this report are assuming steady state conditions, the churning losses can be directly calculated by comparing the energy flux flow in and out of the system or CFD model respectively (energy conservation).

Churning losses = heat convection – heat soak.

By using the above approach, the churning losses were calculated from the CFD predicted energy flux flows for each coupling configuration.

Figure 10 shows the result of the calculated churning losses for the 3 most common configurations using drive bolts, stripper bolts and stripper bolt covers or no windage covers at all.

It can be seen from the results that the losses predicted for all three configurations are similar and more significantly they suggest that the additional windage features do not reduce the overall losses but could increase the losses compared to a coupling without any windage features.

One proposed explanation is that although flow separation at the bolts is reduced by introducing the covers, the additional surface area of the features causes additional drag and therefore eliminates the net gain or even reverses the trend.

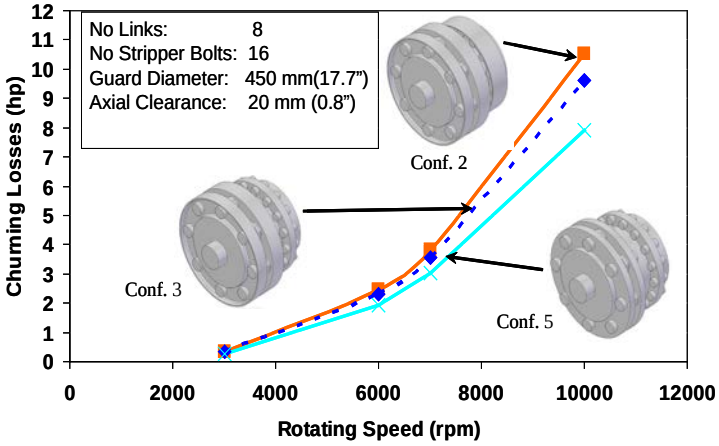


**Figure 10. Predicted churning losses for the coupling with and without windage features.**

Figure 11 shows the maximum predicted guard temperature for the coupling configurations shown in Figure 10.

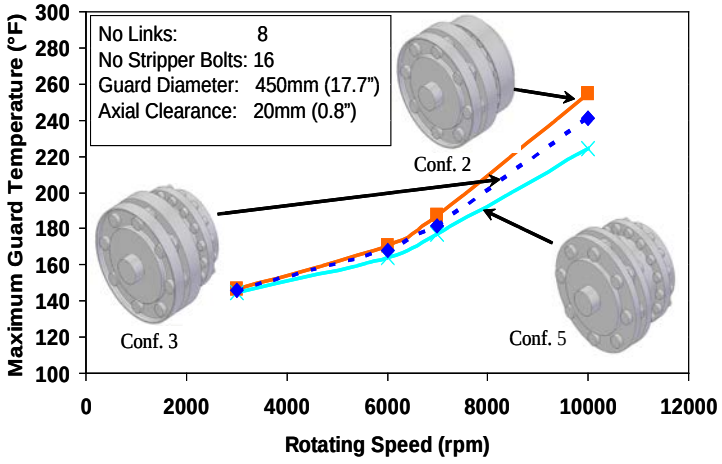


**Figure 11. Predicted maximum guard temperatures for the coupling with and without windage features.**

From Figure 11 it can be seen that the maximum guard temperature is not changing as significantly across the speed range as the change in windage losses (Figure 10) may suggest. The reason for this is that the guard temperature is not only influenced by the losses of the coupling but the environment conditions. At low speed the results are influenced by the estimated and fixed machine casing and bearing/ shaft temperature, which means, the environment is heating the coupling and guard. At high speed some of the heat generated by the coupling through windage conducts through the shaft or by convection into the side wall of the machine casing. Figure 11 also confirms that the additional windage features has a small impact on the guard temperature. The simulation suggests that the lowest guard temperature is achieved for a coupling without the windage features.

## EMPIRICAL VERIFICATION

### *Coupling Testing*

The analytical data has been verified by a series of dynamic tests used to simulate the CFD analysis as close as possible. The test setup consisted of a one half of a coupling connected to the free-end of a dynamic rig capable of rotating at 10,000rpm. The coupling geometry exactly replicated the profile of a high performance coupling design as shown in Figure 1 and included membrane and all flange bolting. The windage features over the bolting was also replicated and had the ability to be easily removed. The assembly was then housed in such a way to simulate a coupling guard as shown in Figure 12, with the clearance set in line with the CFD calculations. To minimize the external influence the spacer end of the assembly (shaft end) was fitted with a mechanical seal which contacted on start up and then bedded in for a non contacting operation. The gap between the membrane flange and the guard at the coupling end was maintained at 20mm although this can be reduced to 3mm to alter the effect of heat sink from external influences.

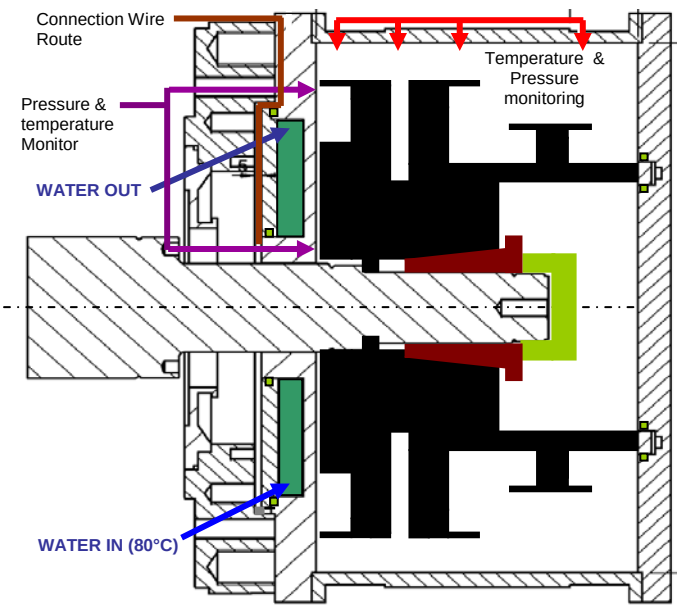


**Figure 12. Test setup.**

To keep the test conditions consistent a heat jacket was fitted which maintained the end of the coupling at 80°C. The pressures and temperatures were monitoring around the assembly and power absorbed at the shaft line. The sensor positions can be seen in Figure 13 and 14.

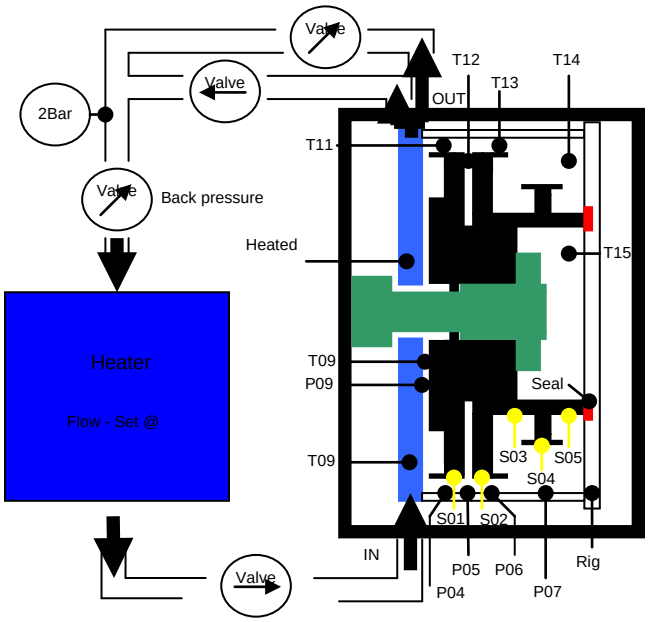


**Figure 13. Rig configuration – schematic & setup.**

T = Thermocouples
P = Pressure Sensors
S = Thermo strips

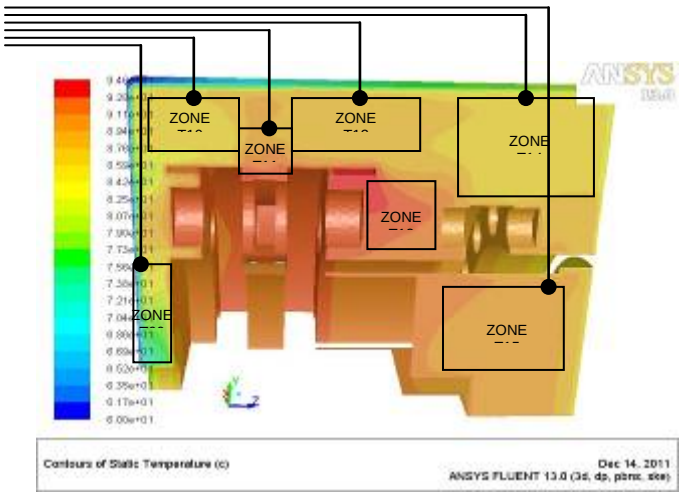


**Figure 14. Zone monitoring.**

The initial plan was to run 5 main configurations:

Configuration 1 – all features fitted, windage flanges, membrane bolt plate (extra feature on high speed design) and membrane windage plate

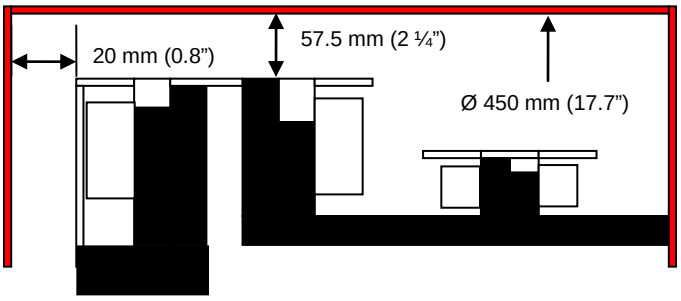


**Figure 15. Configuration 1.**

Configuration 2 – As Configuration 1 but with membrane bolt plate removed.

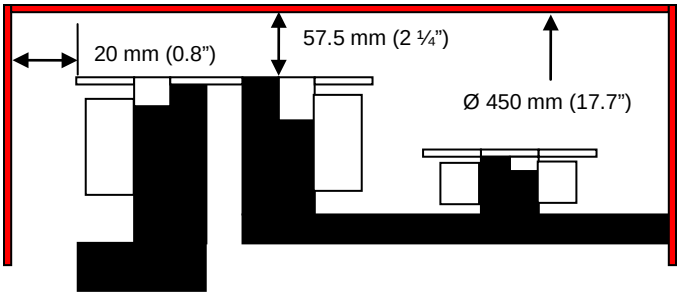


**Figure 16. Configuration 2.**

Configuration 3 –As Configuration 2 but with membrane windage plate removed

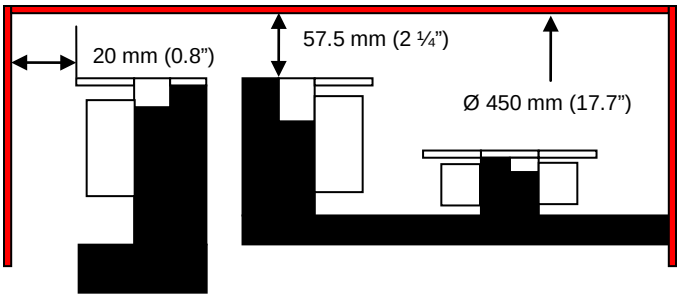


**Figure 17. Configuration 3.**

Configuration 4 – As Configuration 3 but with stripper bolt windage plates removed

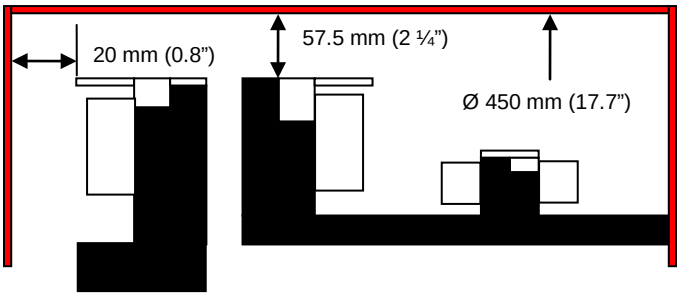


**Figure 18. Configuration 4.**

Configuration 5 – as Configuration 4 but with drive bolt windage plate removed.

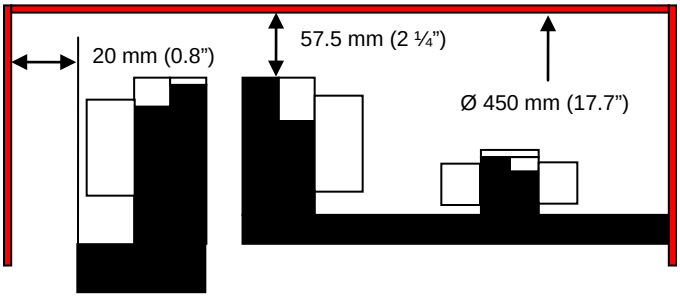


**Figure 19. Configuration 5.**

Due to vibration problems above 7000rpm the test configurations were limited to three setups, configuration 3, 4 and 5. These are shown in Figure 17, 18 and 19 and the actual setup in Figure 20, 21 and 22.

The tests to date confirmed the findings from the CFD simulation, however, when comparing the results from the three test runs, shrouded design versus the coupling with no windage features, it was apparent there was not a significant difference in measured temperature and power absorbed, see Figure 23, confirming the CFD findings that the additional windage features have little impact on the coupling losses. However, the CFD data had also predicted an increase due to the additional surface area of the windage features, which was not replicated in test. Further refinement of the CFD model may be necessary.

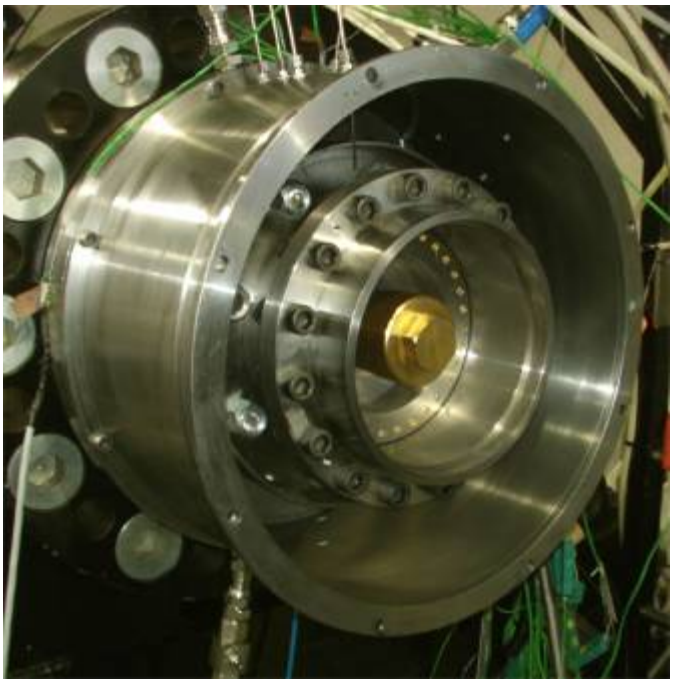

**Figure 20. Test rig guard assembly.**

**Figure 21. Test rig with drive bolt windage feature.**

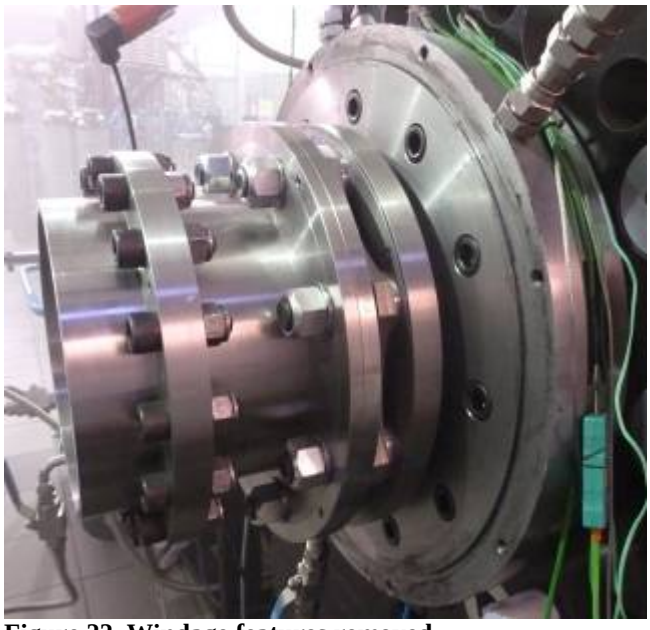

**Figure 22. Windage features removed.**

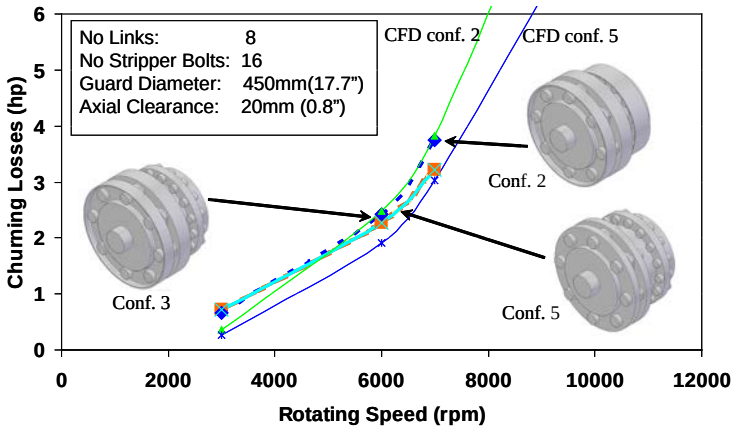


**Figure 23. Summary of results.**

The vibration problem has now been solved and further testing is planned to analyze the effects at 10000rpm using configuration 1 to 5

*Empirical Calculation*

As the correlation of testing and CFD was limited by the critical speed of the existing test configuration to 7000 rpm, the CFD results were compared with the churning loss calculation based on empirical models. These were formulated by Bilgen-Boulos for churning losses for rotating cylinders and Kreith for losses on a rotating disk. Although the empirical calculation is based on a simplistic shape of the coupling (dog bone), which does not take into account small design features such as bolts etc., this calculation method can confirm whether the magnitude of the churning losses resulting from CFD and testing are in the expected range. Figure 24 shows the comparison between CFD, testing and the empirical calculation. The good correlation (deviation < 25%) confirms that CFD and test results to date conform to the classic theory of churning losses.

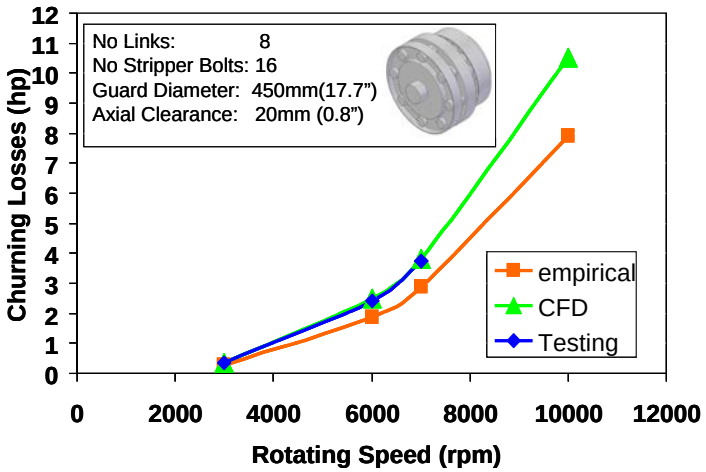


**Figure 24. Comparison of empirical, CFD and testing, configuration 2.**

## CONCLUSIONS

The computational results, supported by limited testing, suggest that conventional windage features are less efficient than generally believed.

Currently the results are limited to one particular coupling design, size and guard design, although this is typical for a high speed turbo machinery applications. Whether the findings can be directly transposed to other coupling designs, sizes and different guard arrangements needs further investigation.

The results to date, however, make a strong case that existing windage features fail to make a significant impact in reducing churning losses and guard temperatures respectively.

The additional costs, weight and component stress concentration from adding conventional windage features is under review as the perceived performance gain is not as significant as first thought, based on testing and CFD.

Further investigation is now required to fully verify the CFD results using a more in-dept test program before a final conclusion can be drawn.

Further studies are now being conducted to review coupling windage in more detail and develop a generic understanding of windage features, covering a wider range of coupling designs. This work will include different guard diameters and air circulation to reduce guard temperatures.

## REFERENCES

Bilgen E. and Boulos R. 1973, "Functional dependence of torque coefficient of coaxial cylinders on gap width and Raynolds numbers," Transaction of ASME, *Journal of Fluids Engineering*, Series I, Vol. 95, No. 1, pp. 122-126.

Kreith F. 1968, "Convection heat transfer in rotating systems," *Advances in Heat Transfer*, Vol 5, Academic Press Inc.: USA, pp. 129-251.

*API Standard 671* Fourth Edition, August 2007, API Publishing Services: USA.